

Maneuver Planning for Conjunction Risk Mitigation with Ground Track Control Requirements

David P. McKinley
a.i. solutions, Inc. Lanham, MD, 20706
david.mckinley@ai-solutions.com

The Earth Observing System (EOS) missions Aqua, Aura, and Terra fly in a relatively high density debris environment. Routine conjunction screening of these missions has taken place since 2004. When a potential conjunction risk is identified for any of these spacecraft, Risk Mitigation Maneuver (RMM) planning is performed. The goal of a RMM is to significantly reduce the probability of collision by increasing the minimum miss distance between the spacecraft and debris object at the Time of Closest Approach (TCA). In addition, the EOS spacecraft are required to fly repeating ground track orbits referenced to the World Reference System - 2 (WRS - 2) and only have the capability to perform posigrade maneuvers. Planning RMMs that also meet the ground track control requirements using only posigrade maneuver capability is challenging and requires a capability to look at a large maneuver trade space.

Originally, RMM planning was accomplished by running the existing EOS high fidelity maneuver planning tool using a range of burn magnitudes. The resulting trajectories were then analyzed to determine the effect of the various maneuvers on the conjunction geometry as well as on the ground track requirements. This process was time-intensive and allowed only a limited set of maneuver options to be evaluated.

However, several key characteristics were observed that led to a simplification of the maneuver trade space. First, the maximum burn duration is primarily driven by the spacecraft's current location in the ground track control box. Unless the spacecraft is at a location in the control box where a routine maneuver would soon be required, the burn magnitudes that maintain the ground track requirements will be small. Second, for small burn magnitudes there is a linear correlation between the conjunction miss distance and RMM magnitude. Additionally, the altitude change from these small maneuvers was found to be inconsequential to changing the overall conjunction geometry, which was instead driven by the change in along-track position resulting from the maneuver. Therefore, the phasing time, or the time between a RMM and the TCA, was observed to be a primary driver in the resulting conjunction geometry.

Given the linear relationship between the miss distance and the maneuver magnitude, it was possible to develop a simple relationship that allows a larger maneuver trade space to be investigated without resorting to multiple runs of the high fidelity maneuver planning tool. Likewise, the maneuver magnitude and phasing time were identified as the key contributors to the resulting conjunction geometry. Equations were developed that determined the along-track change in a spacecraft's position for a given maneuver magnitude and phasing time. The along-track change in the spacecraft position was then used to determine the new conjunction geometry. Additionally, approximate equations

for the maximum WRS – 2 error as a function of burn magnitude were developed. The complete RMM maneuver trade space is then defined as seen in Figure 1. The trade space includes a contour plot of the resulting conjunction miss distance in kilometers for a given phase duration and burn magnitude. Likewise, the approximate maximum WRS – 2 error versus burn magnitude curve is plotted.

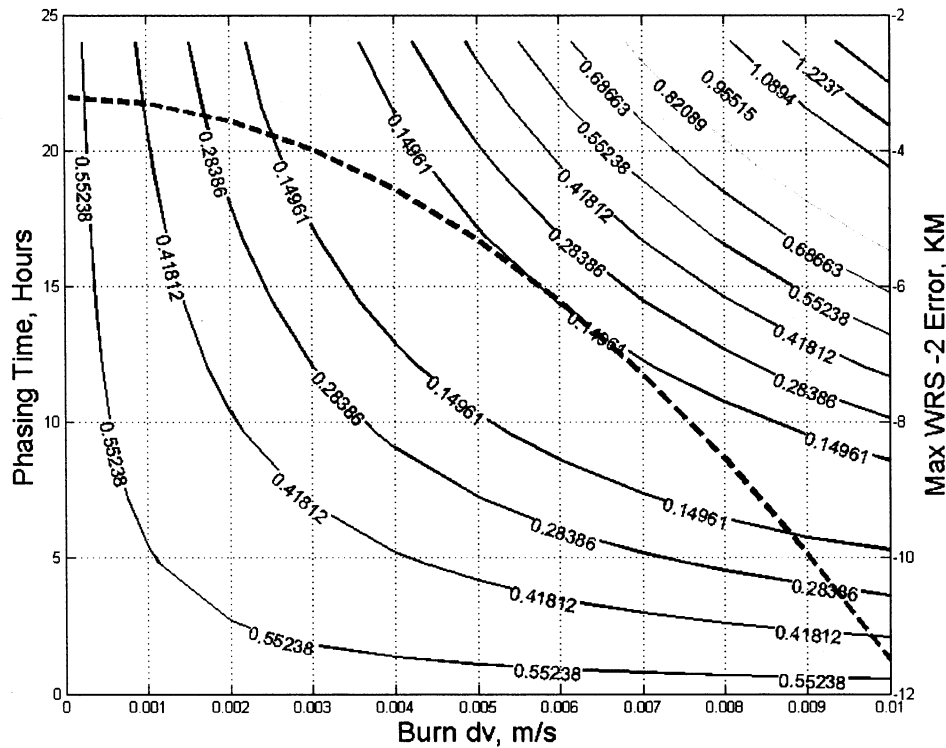


Figure 1. Risk Mitigation Maneuver Trade Space Diagram

The trade space shown in Figure 1 allows the maneuver analyst to get a quick assessment of the magnitudes of maneuvers and phasing durations required to mitigate a potential collision risk while maintaining ground track control requirements. The entire trade space is easily generated using closed form equations, eliminating the need to perform a large number of runs of the high fidelity maneuver planning tool. Instead, the analyst is immediately able to determine the approximate burn duration and phasing for use in the maneuver planning tool. Analyzing options and planning a RMM is often limited by the amount of time available before TCA, and minimizing the analysis time necessary helps to maximize the phasing time available for mitigating the conjunction. This analysis tool is applicable to all spacecraft, and could also be expanded to include any number of additional constraints that are a function of maneuver magnitude.

This paper will derive the analytic equations used to generate the RMM trade space. The assumptions that are made in the derivations will be proven through comparison with the high fidelity maneuver planner. Several representative trade spaces will be shown to demonstrate the utility of the analysis.

Maneuver Planning for Conjunction Risk Mitigation with Ground-track Control Requirements¹

David P. McKinley
a.i. solutions, Inc. Lanham, MD, 20706

Abstract

The planning of conjunction Risk Mitigation Maneuvers (RMM) in the presence of ground-track control requirements is analyzed. Past RMM planning efforts on the Aqua, Aura, and Terra spacecraft have demonstrated that only small maneuvers are available when ground-track control requirements are maintained. Assuming small maneuvers, analytical expressions for the effect of a given maneuver on conjunction geometry are derived. The analytical expressions are used to generate a large trade space for initial RMM design. This trade space represents a significant improvement in initial maneuver planning over existing methods that employ high fidelity maneuver models and propagation.

I. Introduction

Routine conjunction assessment by the Goddard Space Flight Center (GSFC) began in 2005 for the Earth Observing System (EOS) missions Aqua, Aura, and Terra. When a potential conjunction threat is determined by the GFSC Conjunction Assessment (CA) team, spacecraft maneuvers are planned to mitigate the risk. Since 2005, two Risk Mitigation Maneuvers (RMMs) have been performed on the EOS missions. RMMs were performed on the Terra spacecraft in October of 2005 and June 2007. In addition to the two executed maneuvers, RMMs have been planned approximately six more times but were not performed because the conjunctions were eventually deemed to not be a threat. The experience gained planning these RMMs demonstrated a need to streamline the process.

The risk associated with a potential conjunction is typically mitigated by increasing the miss distance between the spacecraft and the debris object by executing a maneuver. The miss distance is the minimum range between the spacecraft asset and the debris object which occurs at the Time of Closest Approach (TCA). Several papers have been written that investigate this problem (1,2). However, the Aqua, Aura, and Terra spacecraft have additional maneuver constraints. First, each of these spacecraft maintains a repeating ground-track orbit such that it flies over the same point on the Earth approximately every 16 days. The ground-track error is measured relative to a predefined set of nodes on the Earth's surface and is maintained by controlling the period of the orbit through the semi-major axis (SMA). The exact repeat ground-track is flown by maintaining an ideal SMA. However, drag causes decay from the ideal SMA and routine maneuvers are required to increase the SMA. Additional information on EOS mission ground-track control can be found in (3). The design of the propulsion systems and thermal constraints on the

¹ This paper was supported by the National Aeronautics and Space Administration (NASA)/Goddard Space Flight Center (GSFC), Greenbelt, MD, under MOMS contract (NNG04DA01C), Task Orders #209

spacecraft determines that only posigrade maneuvers are possible for orbit maintenance and therefore RMMs. Additionally, the tight ground-track control requirements (± 20 km at the node) require that relatively small maneuvers be performed. To date, the largest posigrade maneuver performed by the Terra spacecraft was only 0.24 m/s.

In this investigation, the fact that only small, posigrade maneuvers are typically available for RMM on Aqua, Aura, and Terra is used to derive analytical expressions for the effect of a maneuver on conjunction geometry under these circumstances. This information is combined with equations for ground-track control to develop a Risk Mitigation Maneuver Trade Space. This Trade Space allows a wide variety of RMM options to be considered and the effect of those maneuvers on ground-track control to be analyzed.

II. Observations from Current Maneuver Planning Process

Currently, when a potential conjunction is determined to be a threat to an asset, the information is relayed by the Conjunction Assessment team to the EOS Flight Dynamics team to begin maneuver planning. The current RMM planning process for Aqua, Aura, and Terra spacecraft uses the existing Drag Make Up (DMU) maneuver targeting tools in the EOS Flight Dynamics System (FDS). These tools were designed to target posigrade maneuvers to maintain ground-track requirements. The FDS maneuver targeting tools use numerical integration of the spacecraft models to target a specific minimum ground-track error and produce required command products to perform the maneuver. For routine DMU maneuvers, the maneuver time is determined at least two weeks in advance, and the actual maneuver planning is done over a two-day period.

The conjunction assessment process typically identifies possible threats up to seven days in the future. The determination of a conjunction as an actual threat is typically made only two to three days prior to the conjunction TCA after collecting data on the conjunction for several days. However, for a small RMM to be effective, the maneuver must be performed as far before the TCA as possible. In addition to choosing an effective maneuver, other operational constraints must be met, such as the maneuver analyst and the Flight Operations Team need to identify available maneuver times, schedule network resources, and build maneuver plans and products. Therefore, when planning a RMM, the amount of time available to perform the analysis is often limited, and the maneuver execution time is often driven by these external operations constraints.

As a first guess, the maneuver analyst typically targets the largest possible burn that maintains the ground-track requirement. The resulting trajectory is then delivered to the CA team who performs analysis to determine if the maneuver will mitigate the threat. If the CA team determines the threat is not sufficiently mitigated, the procedure is repeated with a larger burn targeted. If the first-guess burn is larger than required to mitigate the threat, the maneuver may be retargeted to be smaller and therefore provide margin in the ground-track control box. Using this operational EOS maneuver planning process to plan the RMM is time-consuming, since the maneuver planning tool uses high fidelity numerical propagation to target the maneuver. Obviously, this iterative process is

inefficient and necessitates a method to determine a better initial maneuver estimate than simply targeting the limits of the control box.

Two key observations have been made based on past RMM planning experience. First, given the small magnitude of typical ground-track maneuvers, changes in the radial position of the spacecraft are not significant contributors to the overall change in the spacecraft's position. The dominant change in the spacecraft's position is in the in-track components and is achieved via phase drift resulting from the change in the SMA of the orbit. When a posigrade maneuver is performed, the period of the spacecraft is increased while the orbital velocity decreases. Therefore, the spacecraft will then drift in the in-track direction relative to its original trajectory. The amount of drift, called the phase, is a function of the change in mean motion of the orbit and the time over which the spacecraft phases, or phasing time. This observation means that when designing a RMM, not only is the size of the maneuver important, but also the time between the RMM and the TCA, called the phasing time. Adequate separation may be achieved between the asset and debris object at TCA with a small maneuver if sufficient phasing time is available before the conjunction. However, because the timing of a maneuver before the TCA of a conjunction is often constrained by operational considerations (e.g. network resource scheduling), larger maneuvers may be required to achieve separation when the maneuver can only be performed "close" to the TCA.

The second observation was made by plotting the in-track and cross-track miss distance components versus maneuver duration. The in-track and cross-track miss distance components for a particular conjunction are shown in Figure 1. For this conjunction the in-track and cross-track miss distance components were reported to be approximately -500 meters and -390 meters at the TCA respectively and are shown on the plot as the 0 second Burn Duration point. The maneuver options were planned at the TCA - 24 hour point. It is seen that the in-track and cross-track components vary linearly with maneuver duration (or magnitude) for a given phasing time. While Figure 1 shows only one example of the linear behavior of the miss distance components with burn duration, this relationship has been observed on all RMMs planned to date.

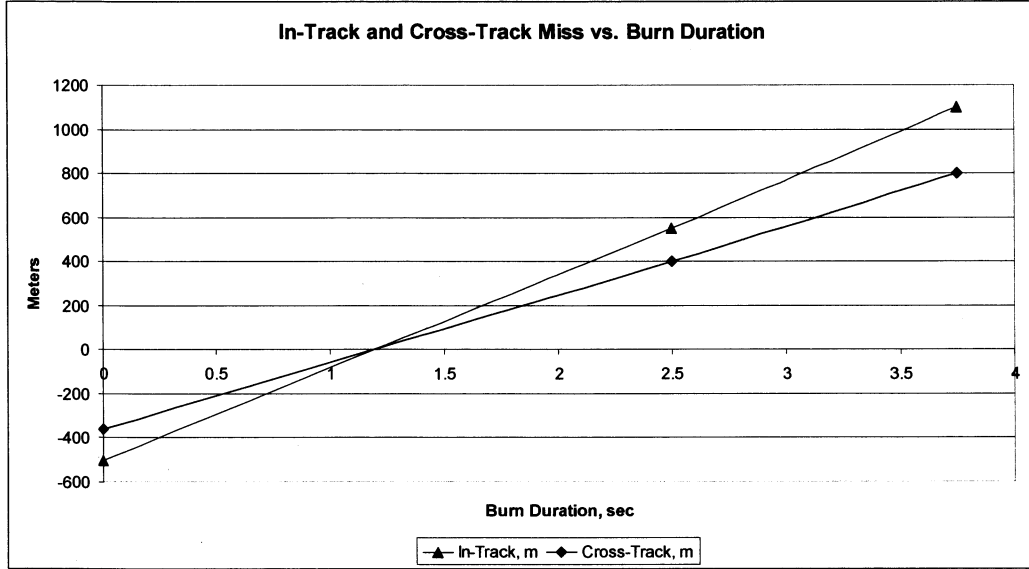


Figure 1. In-track and cross-track components of miss distance versus maneuver duration.

Given that the behavior of the resulting miss distance components is linear with burn magnitude, and that the miss distance is driven primarily by in-track phasing, it was assumed that an analytical expression could be derived that would relate the burn magnitude and phasing time to a resulting miss distance for a given conjunction. Using an analytical expression, a larger maneuver trade space could be quickly explored and initial maneuver estimates made without resorting to using the high fidelity maneuver targeting tools. The derivations of these analytical expressions are shown in the next section.

III. Analysis

The first observation in the previous section was that the miss distance of a conjunction at TCA is increased primarily via changes in the in-track position of the spacecraft caused by the maneuver executed at some time before the TCA. Therefore, the first step in the analysis is to determine how an applied change in velocity will affect the in-track position of the spacecraft as a function of the phasing time, or time between the RMM and TCA. For a nearly circular orbit, the arc distance the spacecraft will travel over in a given period of time is a function of the mean motion and radius of the orbit:

$$I(t) = RnT = R\sqrt{\frac{\mu}{a^3}}T \quad (1)$$

In Equation 1 $I(t)$ is the in-track distance traveled, R is the orbital radius, n is the mean motion of the orbit, μ is the gravitational parameter of the Earth, a is the SMA of the orbit, and T is the time of flight or phasing time. The change in in-track position as a function of change in the orbit energy can be found by taking the derivative of Equation 1 with respect to the SMA. It is also assumed that the changes in the SMA will be small

compared to the radius of the orbit, so R is held constant. The resulting derivative of the in-track position versus SMA is:

$$\frac{dI(t)}{da} = -\frac{3}{2}RT\sqrt{\frac{\mu}{a^5}} \quad (2)$$

The vis-viva equation for an arbitrary orbit produces the relationship between the SMA and the orbit radius and velocity, v , given by

$$a = \frac{\mu R}{2\mu - Rv^2} \quad (3)$$

Taking the derivative of Equation (3) with respect to velocity and assuming a circular orbit such that $v = \sqrt{\mu/a}$ and $R \approx a$ gives an expression for the change in SMA for a given change in velocity as

$$\frac{da}{dv} = 2\sqrt{\frac{a^3}{\mu}} \quad (4)$$

Equations 2 and 4 can now be combined and the derivative operators transformed to delta operators to give

$$\Delta I(T) = -3\Delta v T \quad (5)$$

Equation (5) states that the change in the in-track position of a spacecraft due to a maneuver is simply a function of the magnitude of the maneuver and the time T . It should be remembered that the velocity change used in this derivation is assumed to be entirely posigrade, or in the in-track direction. The time in Equation (5) is equivalent to the phasing time discussed in the previous section.

The simple derivation given above is easily verified via the Clohessey-Wiltshire (CW) Equations. The CW equation for the in-track component is given by:

$$y(t) = \left(6x_0 + \frac{4\dot{y}_0}{\omega}\right)\sin\omega t + \frac{2\dot{x}_0}{\omega}\cos\omega t - (6\omega x_0 + 3\dot{y}_0)t + \left(y_0 - \frac{2\dot{x}_0}{\omega}\right) \quad (6)$$

In Equation 6, x is in the radial direction, y is in the in-track direction, and ω is the mean motion of the orbit. For the problem we are interested in, all the initial positions are zero. Also, since the maneuvers under investigation are strictly posigrade, the only non-zero initial rate is \dot{y}_0 . Therefore, Equation (6) reduces to:

$$y(t) = \left(\frac{4\dot{y}_0}{\omega}\right)\sin\omega t - 3\dot{y}_0 t \quad (7)$$

The linear term in Equation 7 matches that derived in Equation 5. The periodic term in Equation 7 does not contribute significantly when compared to the linear term and can therefore be ignored.

Equation 5 provides the change in the in-track position at TCA of the maneuvering spacecraft as a function of maneuver magnitude, Δv and phasing time, T . We now need to relate this change in in-track position caused by the RMM to the change in miss distance at TCA for the conjunction. This change in the miss distance at TCA is due to the fact that the maneuvering spacecraft has shifted in the in-track direction due to the RMM by the amount determined by Equation 5. This in-track shift effectively changes the geometry of the conjunction as will be demonstrated next.

The original, non-maneuver orbital position and velocity vectors for the asset and debris object at TCA are known: $\vec{R}_a, \vec{V}_a, \vec{R}_d, \vec{V}_d$. It is assumed that for the small burn magnitudes available that the TCA of the conjunction will not shift significantly. Also, it is assumed that the encounter between the asset and debris object has a high relative velocity, and the relative motion between the two objects in the problem can be treated as linear. Also, it is assumed that the orbits involved are circular so that all in-track motion is in the direction of the velocity vector. Therefore, after the maneuver, the velocity of the asset has been increased by the size of the maneuver in the direction of the velocity vector due to the circular orbit assumption and limiting burn types to posigrade maneuvers. The position vector of the asset is also changed by the in-track position calculated in Equation 5. Since the orbits are assumed to be circular, the in-track direction of the asset's orbit is defined by the orbital velocity vector. Therefore, the change in the asset's position at TCA will have a magnitude defined by Equation 5 and will be applied in the direction of the new velocity vector. Therefore, the changes to the assets position and velocity at TCA after a maneuver with magnitude Δv and phasing time T can be written as:

$$\begin{aligned} {}^+\vec{V}_a &= \vec{V}_a + \Delta v \hat{V}_a \\ {}^+\vec{R}_a &= \vec{R}_a - 3\Delta v T {}^+\vec{V}_a \end{aligned} \quad (8)$$

In Equation 8, the “+” superscript denotes the post-maneuver value. Equation 9 now gives the post-maneuver position and velocity vectors of the asset at the original TCA as a function of the maneuver magnitude and phasing time. The maneuver will have changed the relative geometry of the conjunction, so the new, post-maneuver TCA must be found. The relative position and velocity vectors between the asset and debris object are given by

$$\begin{aligned} \vec{R}_{\text{Rel}} &= \vec{R}_d - {}^+\vec{R}_a \\ \vec{V}_{\text{Rel}} &= \vec{V}_d - {}^+\vec{V}_a \end{aligned} \quad (9)$$

Under the assumption of linear relative motion the new, post-maneuver TCA will occur when the relative velocity is perpendicular to the relative position. The relative position as a function of time can be approximated linearly as

$$\vec{R}_{Rel}(t) = \vec{R}_{Rel} + \vec{V}_{Rel}t \quad (10)$$

Taking the dot product of Equation 10 with the relative velocity and solving for the time when the dot product goes to zero gives

$$t_{TCA} = -\frac{\vec{R}_{Rel} \cdot \vec{V}_{Rel}}{V_{rel}^2} \quad (11)$$

Equation 11 solves for the time change in the TCA resulting from the maneuver. The miss distance at the new TCA is then found by substitution of Equation 11 into Equation 10:

$$\vec{R}_{miss} = \vec{R}_{Rel} - \vec{V}_{Rel} \frac{\vec{R}_{Rel} \cdot \vec{V}_{Rel}}{V_{rel}^2} \quad (12)$$

The final scalar miss distance is the RSS of Equation 12.

The previous analysis provides an analytical method for calculating the miss distance that results from a given burn magnitude and phasing time. The analytical method was tested versus full numerical propagation for an 18-hour and 36-hour phasing time which were two available maneuver times for this particular conjunction. The results of this comparison are shown in Table 1. The original miss distance for this conjunction was 406 kilometers with the maneuvering asset originally in front of the debris object in the in-track direction. Therefore, any posigrade burn initially decreases the miss distance between the two objects. Table 1 demonstrates that the new analytical method agrees very well with the full propagation. The maximum difference between the two methods is less than 2%. This level of agreement between the method derived in the paper and numerical propagation has been observed on a number of conjunctions.

Table 1. Comparison of new analytical method to determine miss distance versus propagation.

Delta-V m/s	Phase Duration, Hours	Propagated Miss Distance, km	Analytic Miss Distance, km	% Error
0.001	18	0.330	0.332	-0.606
1.001	18	157.906	156.517	0.880
2.001	18	316.255	313.344	0.920
3.001	18	474.685	470.150	0.955
4.001	18	633.166	626.936	0.984
5.001	18	791.668	783.701	1.006
6.001	18	950.160	940.444	1.023
7.001	18	1108.611	1097.167	1.032
8.001	18	1266.991	1253.869	1.036
9.001	18	1425.269	1410.550	1.033
0.001	36	0.172	0.174	-1.163
1.001	36	316.005	313.521	0.786
2.001	36	632.201	627.176	0.795
3.001	36	948.171	940.789	0.779
4.001	36	1263.675	1254.436	0.731
5.001	36	1578.470	1567.889	0.670
6.001	36	1892.315	1881.377	0.578
7.001	36	2204.968	2194.822	0.460
8.001	36	2516.190	2508.226	0.317
9.001	36	2825.741	2821.587	0.147

For the EOS missions, the maneuver magnitude is limited by the ground-track control requirements. An analytical expression for the ground-track error is given by (4)

$$\Delta\lambda(t) = \Delta\lambda_0 + \left(\Delta\dot{\lambda}_0 - 3\omega_e \frac{\Delta v}{V} \right) t + \frac{3}{4} V \omega_e \beta \rho t^2 \quad (13)$$

Here $\Delta\lambda$ is the ground-track error at the node, $\Delta\dot{\lambda}$ is the ground-track error rate, ω_e is the rotational rate of the earth, V is the orbital velocity of the spacecraft, β is the ballistic coefficient, and ρ is the atmospheric density. Taking the derivative of the ground-track error with respect to time and setting it equal to zero allows us to find the time to the maximum ground-track error as

$$t_{\max} = \frac{2}{3\omega_e \beta \rho V} \left(3\omega_e \frac{\Delta v}{V} - \Delta\dot{\lambda}_0 \right) \quad (14)$$

Substitution of Equation 14 into Equation 13 gives an analytical expression for the maximum ground-track error as a function of maneuver magnitude and drag environment. A comparison of the analytical ground-track error given by Equations 13 and 14 was compared to a numerical propagation for several cases, and the results are shown in Table 2. The initial ground-track error was -3.2 kilometers, the initial error rate was -0.02 km/day, the ballistic coefficient was 2.23e-8 and the atmospheric density was

$1.84\text{e-}8 \text{ kg/km}^3$. Table 2 shows that while not precise, the analytical approximation does determine the maximum ground-track error within a few kilometers. The accuracy of this method is highly dependent on the ability to predict the average atmospheric density over the time of interest and in determining the initial conditions on the ground-track error and rate. However, the speed of the analytic method over the full propagation makes it very useful in initial maneuver assessment.

Table 2. Comparison of analytic method to determine ground-track error versus propagation.

Delta-V m/s	Propagated Ground Track Error, km	Analytic Ground Track Error, km
0.010	-3.8	-4.1
0.025	-7.1	-8
0.050	-18.9	-21.7

IV. Maneuver Trade Space

The previous section developed analytical expressions for the miss distance at TCA resulting from a RMM as a function of maneuver magnitude and phasing time as well as maximum ground-track error as a function of maneuver magnitude under the following assumptions:

- Maneuvering spacecraft has a nearly circular orbit
- Maneuver magnitude is small such that changes in SMA are small compared to the orbital radius
- Maneuver direction is entirely in the in-track direction
- The conjunction has a high relative velocity so that the motion between the asset and debris object can be assumed to be linear during the encounter

It is now straightforward to use the equations developed and present the results graphically in a maneuver trade space. The RMM Trade Space will be unique for each conjunction and requires the orbital position and velocity of the asset and debris object at TCA for construction. For a range of maneuver magnitudes and phasing duration Equation 5 is first used to determine the change in in-track position of the maneuvering spacecraft. Equations 8 – 12 are then used to determine the change in the conjunction miss distance from this change in in-track position. The result is a trade space of miss distance as a function of burn magnitude and phasing time. Likewise, Equation 13 and 14 are used to determine the maximum ground-track error as a function of burn duration. This trade space presents the two important factors in RMM planning for EOS missions - miss distance increase and ground-track control error - in a single, easy to generate product.

A sample RMM Trade Space is presented in Figure 2. The initial miss distance for the conjunction analyzed here was approximately 500 meters. The post RMM miss distance at TCA as a function of maneuver magnitude and phasing time is presented as a contour

plot with the phasing time on the left-hand vertical axis and the maneuver magnitude presented on the horizontal axis. To determine the miss distance resulting from an RMM with a given magnitude and phasing time, the analyst would find where on the contour plot the maneuver magnitude and phasing time intersect. For example, a 0.009 m/s maneuver performed 20 hours before TCA results in approximately 1.1 km miss distance. Presenting the miss distance as a contour plot is natural given the two variables, burn duration and phasing time, in the derivation. Also, the contour plot shows important features of the conjunction geometry. For example, in Figure 2 it is immediately observed that there is a “trough” in the miss distance associated with the fact that the maneuvering asset initially is in-front of the debris object in the in-track direction. The available posigrade burns put the asset into a higher orbit with a slower period so that the asset will initially phase toward the debris object. This result is an important consideration in RMM design because it reveals that certain burn magnitudes and phasing time combinations actually decrease the miss distance. Understanding this geometry is extremely important in designing RMM.

The right-hand vertical axis of the RMM Trade Space plots the maximum ground-track error as a function of burn duration calculated from Equations 13 and 14. The ground-track error is shown on the plot as the dashed line. Plotting this curve gives the maneuver designer immediate insight into the effect of a maneuver on the ground-track control requirements. For the 0.009 m/s burn used in the example above, the resulting ground-track error would be approximately -9 km.

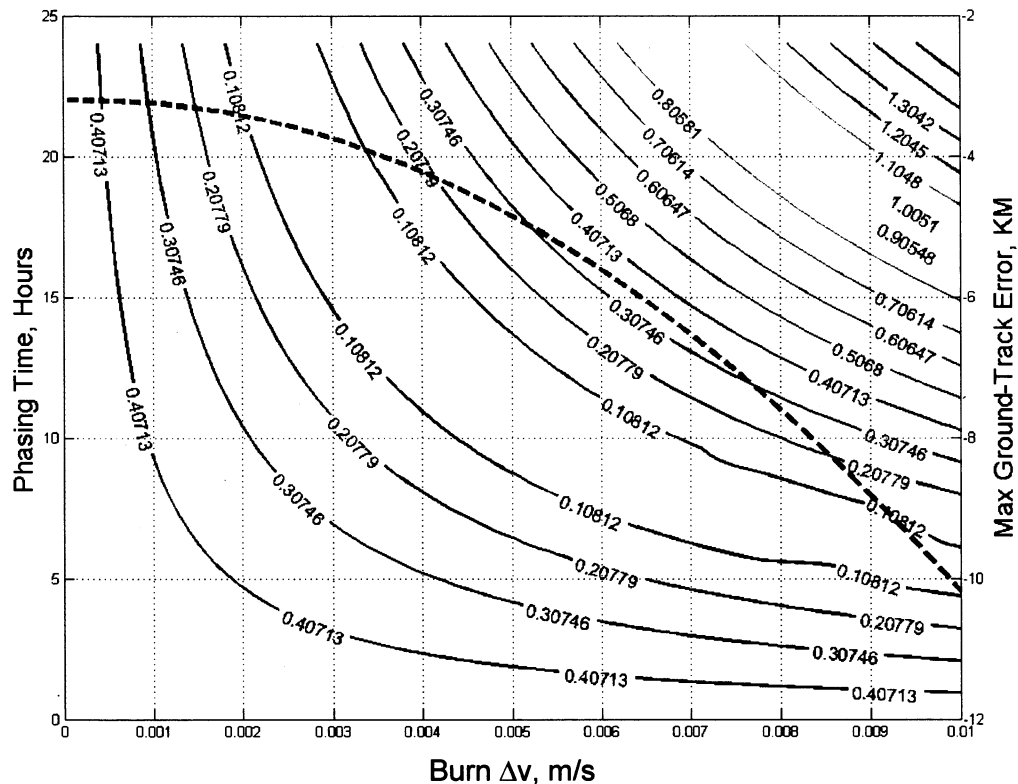


Figure 2. Risk Mitigation Maneuver Trade Space. Miss Distance in Km.

There are several distinct advantages to using the equations developed in the paper to present the RMM Trade Space as shown in Figure 2. The most important advantage is that the Trade Space is developed using closed-form equations. This greatly improves the volume of maneuver options that can be initially considered. RMM planning typically takes place under considerable pressure where maneuver planning, command product generation, resource scheduling, and spacecraft commanding may all take place outside of the normal operations plan. The RMM Trade Space allows the maneuver designer to bring multiple options to the flight operations team and mission management immediately for discussion. Second, the RMM Trade Space provides all of the key maneuver constraints in a single plot to aid decision making. For example, if network resources dictated that a maneuver must be performed at the TCA – 20 hour point, Figure 2 immediately shows that a maneuver greater than 0.005 m/s must be performed to increase the miss distance over the no-burn case which has a miss distance of 400 meters. Likewise, if the maximum ground-track error requirement is -10 km, it is immediately seen that the largest possible burn is 0.01 m/s. The ability to generate and present this large quantity of information quickly and without time consuming propagation of spacecraft models will greatly increase operational responsiveness to potential conjunction threats.

V. Conclusion

To date, the Risk Mitigation Maneuver planning for the EOS spacecraft Aqua, Aura, and Terra has been accomplished by running the existing operational ground-track control targeting software to generate candidate maneuvers. This process involves numerical propagation of the spacecraft and maneuver models, which can be time consuming and limits the number of maneuver options that can be investigated. This investigation derived analytical expressions for the effect of maneuver magnitude and phasing time on the conjunction geometry. Additionally, the analytical expressions for the ground-track control error are derived. These equations are then used to generate a RMM Trade Space which provides both conjunction miss distance as a function of maneuver magnitude and phasing time and ground-track error as a function of maneuver magnitude. This trade space can be used to quickly identify RMM candidates while also considering other operational constraints such as network resources.

Extensions of this RMM Trade Space are possible. Given adequate information on the post maneuver uncertainty, the trade space could be presented in terms of Probability of Collision rather than miss distance. Additionally, any orbital constraint that can be written as a function of maneuver magnitude, such as SMA, can be used instead of the ground-track error control which is important to the EOS missions but may not be important for others. Finally, while the RMM Trade Space was developed for Aqua, Aura, and Terra maneuver planning, the techniques developed here can be used for any spacecraft that meets the assumptions outlined in the analysis. The only information required to generate the RMM Trade Space are the asset and debris object position and velocity states at the TCA of the conjunction. For spacecraft with larger maneuver

capability or eccentric orbits, further analysis is required to see if/when the assumptions in this analysis break down.

References

1. Foster, J., "The Analytical Basis for Debris Avoidance Operations for the International Space Station and Space Shuttle," *Orbital Debris Quarterly News*, Vol. 6, No. 2, 2001, p. 11.
2. Patera, R., and Peterson, G., "Space Vehicle Maneuver Method to Lower Collision Risk to an Acceptable Level," *Journal of Guidance, Control, and Dynamics*, Vol. 26, No. 2, 2003, p. 233 – 237.
3. Demarest, P., Richon, K., Wright, F., "Analysis For Monitoring the Earth Science Afternoon Constellation," AAS 05-368, 2005, AAS/AIAA Astrodynamics Specialist Conference, Lake Tahoe, Ca., August 2005.
4. Bhat, R. S., Frauenholz, R. B., Cannell, R. E., "TOPEX/POSEIDON Orbit Maintenance Maneuver Design," AAS 89-408, 1989, AAS/AIAA Astrodynamics Specialist Conference, Stowe, Vt., August 1989.